

# Interfacial Heat Transfer Measurements during Flow Boiling in a PDMS Rectangular Microchannel

Sofia KORNILIOU<sup>1,\*</sup>, Coinneach M. DOVER<sup>2</sup>, Anthony J. WALTON<sup>2</sup>, Souad HARMAND<sup>4</sup>, Tassos G. KARAYIANNIS<sup>1</sup>, Khellil SEFIANE<sup>3</sup>

\* Corresponding author: Email: sofia.korniliou@brunel.ac.uk

<sup>1</sup> Department of Mechanical and Aerospace Engineering, Brunel University London, UB8 3PH, UK

<sup>2</sup> Institute for Micro and Nano Systems, School of Engineering, SMC, Alexander Crum Brown Road, Edinburgh, EH9 3FF, UK

<sup>3</sup> Institute for Multiscale Thermofluids, School of Engineering, University of Edinburgh, King's Buildings, Edinburgh EH9 3DW, UK

<sup>4</sup> UVHC, LAMIH/ CNRS8201, Valenciennes 59313, France

**Keywords:** Flow boiling, transparent heating, microchannel, infrared thermography, pressure sensors

**Abstract:** Flow boiling heat transfer rates and associated thermal and flow patterns were experimentally investigated using interfacial wall temperature mapping with synchronised high-speed visualisation and pressure measurements from integrated pressure sensors in a Polydimethylsiloxane (PDMS) microchannel. Flow boiling experiments were performed in a single high aspect ratio transparent microchannel of width  $W_{ch} = 2.26$  mm and height  $H_{ch} = 100$   $\mu\text{m}$  giving a hydraulic diameter  $D_h = 192$   $\mu\text{m}$  using FC-72. The mass flux values studied were 23.59, 36.87, 73.74 and 101.62  $\text{kg m}^{-2} \text{s}^{-1}$  and heat flux was up to 98  $\text{kW m}^{-2}$ . The transient two-dimensional (2D) wall temperature maps recorded by a high-speed infrared camera were used to calculate the heat transfer coefficient at the inner wall of the microchannel. Then, the local heat transfer coefficients were correlated with simultaneous high-speed video optical images obtained from the channel base. The 2D two-phase heat transfer coefficients  $h_{in}(x, y)$  are reported as a function of time in 3D plots. 3D plots of the local heat transfer coefficient fluctuations are presented for the onset of boiling (ONB), maximum heat transfer coefficient ( $\text{HTC}_{\text{max}}$ ) and critical heat flux (CHF). The heat transfer deterioration that occurred in microchannels was associated with liquid film thinning during annular flow that leads to local and temporal dryout.

## 1 Introduction

Flow boiling heat transfer coefficients in microchannels to the prevailing flow patterns. The relationship between heat transfer coefficient and flow patterns should be understood in order to develop heat transfer correlations based on flow patterns along the channel [1]. As the bubbles grow in the microchannel they occupy the channel cross section and can alter the liquid-vapour distribution on the channel surface. Wide or high aspect ratio ( $a = W_{ch}/H_{ch}$ ) microchannels are expected to provide high heat transfer coefficients because of their large surface-to volume ratio and the amount of liquid retained in their corners and shorter sides. It has been reported that they promote elongated bubbles [2] with the associate liquid film between the bubbles and the wall. New methods are required in order to investigate liquid film thinning that can induce early heat transfer deterioration in a microchannel when it dries up. Wall temperature 2D mapping using nonintrusive infrared thermography (IR) allows the measurement of the rapid changes of temperature with time as a function of channel length and width during the transition of flow patterns. So far, most researchers acquired temperature measurements from the outer wall of the channel, allowing later for thermal conduction [2]. This study uses a Polydimethylsiloxane (PDMS) microchannel which is transparent to midwave infrared (IR) in order to give a better insight into evaporation heat transfer at the wall-fluid interface. The simultaneous local pressure measurements were used in order to calculate the local heat transfer coefficients. Simultaneous flow visualisation from the transparent indium tin oxide (ITO) base was also carried out.

## 2 Experimental Method

Figure 1 shows a schematic of the test section and the position of the infrared and high-speed camera with reference to the microchannel. A flow loop system was designed to circulate degassed FC-72 into the test section, which was later collected in the reservoir. The

transparent test section was a rectangular microchannel fabricated from PDMS (transparent to infrared) with a hydraulic diameter of  $D_h = 192$   $\mu\text{m}$ , length ( $L$ ) of 20 mm and aspect ratio ( $a$ ) of 22. Two piezoresistive pressure sensors were integrated near the inlet and outlet of the channel. The microchannel was bonded on a glass slide coated with indium tin oxide (ITO) for Joule heating. In situ calibration of the surface emissivity was carried out. Details for the experimental setup can be found in previous study of Korniliou *et al.* [3].

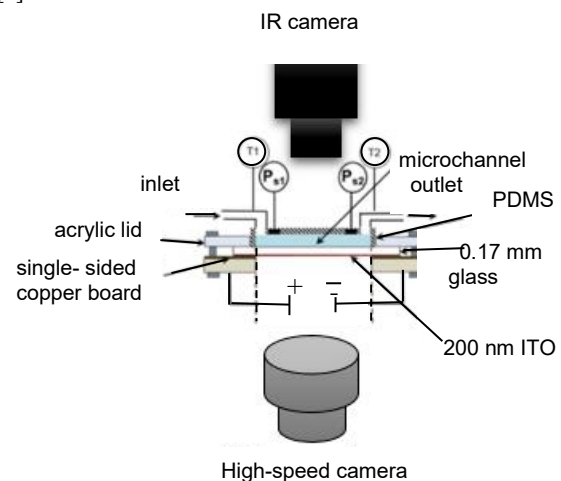
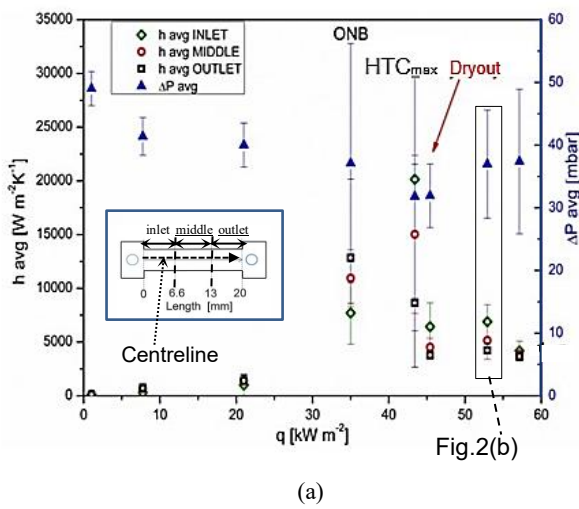


**Figure 1.** Schematic drawing of the test section side view.

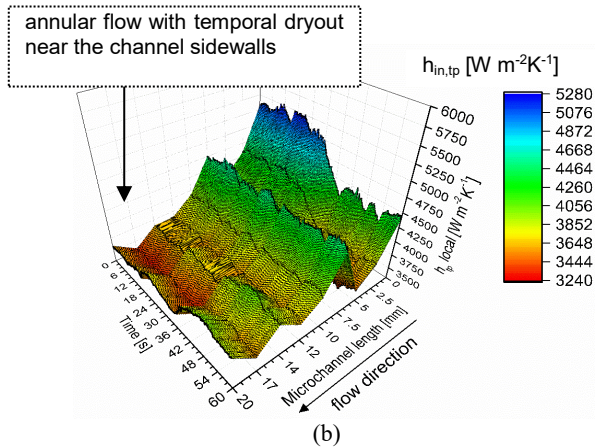
Flow observations at the heated base and pressure measurements were obtained from pressure sensors inside the microchannel, simultaneously with the thermal images. Two-dimensional temperature  $T_w(x, y)$  at the channel interface, local pressure and heat transfer data were produced for the mass fluxes of 23.59, 36.87, 73.74 and 101.62  $\text{kg m}^{-2} \text{s}^{-1}$  and heat fluxes up to 98  $\text{kW m}^{-2}$ .

### 3 Results and discussion

This section presents 3D plots of local heat transfer coefficients as a function of time for  $G=23.59, 36.87, 73.74$  and  $110.62 \text{ kg m}^{-2}\text{s}^{-1}$  at a range of heat fluxes. Figure 2(a) shows a 2D plot with time averaged and spatially averaged heat transfer coefficients at the channel centerline for the inlet, middle and outlet of the microchannel and local pressure drop averaged within the time as function of heat flux. The local pressure drop was calculated using the pressure measurements from the pressure sensors ( $P_{s1}, P_{s2}$ ) located inside the microchannel (see Figure 1).  $h_{avg}$  increases with increasing heat flux up to  $q=43 \text{ kW m}^{-2}$  and then decreases with heat flux. This trend was observed for mass fluxes less than  $73.74 \text{ kg m}^{-2}\text{s}^{-1}$ . 3D plots of local heat transfer coefficients with time revealed the magnitude of the fluctuations that occur during the ONB, maximum heat transfer coefficient ( $HTC_{max}$ ) and CHF. The heat transfer is reduced by transient dryout of the thin film during the annular flow regime, see Figure 2(b). The periodic evaporation of the thin liquid film during annular flow or the passage of long confined bubbles can be deduced from the images of the thermal patterns as shown in in Figure 3.



(a)



(b)

**Figure 2.** (a) Averaged heat transfer coefficients and channel pressure drop for  $G=36.87 \text{ kg m}^{-2} \text{ s}^{-1}$  and increasing heat flux up to  $58 \text{ kW m}^{-2}$  and (b) local heat transfer coefficients at nine equally spaced positions along the whole channel centerline, see Figure 2 (a) averaged two-phase heat transfer coefficients and pressure drop for  $q=58 \text{ kW m}^{-2}$ .

Flow boiling heat transfer during single bubble growth and bubble confinement was evaluated for the lowest mass flux of  $23.59 \text{ kg m}^{-2} \text{ s}^{-1}$ . Figure 4 shows the interfacial wall temperature  $T_w$ , at centreline as a function of channel length and time, from single bubble nucleation to elongated bubble. As seen in the figure temperature presents a decrease at the positions where the bubble is

growing. For example, at  $t=0 \text{ s}$  bubble base has a temperature of  $60.62 \text{ }^\circ\text{C}$ . As the bubble begins to grow the wall temperature underneath it is reduced. The same happens as the bubble elongates, i.e. the wall temperature diminishes with time, see Figure 4.

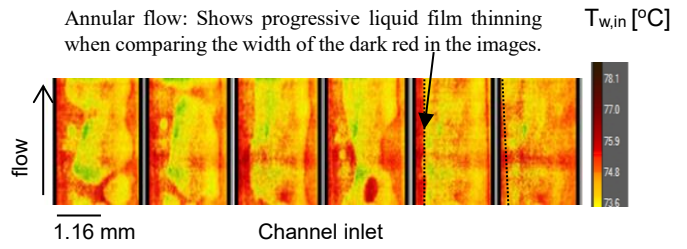


**Figure 3.** Sequence of thermal images obtained at the channel inlet from the PDMS side of the channel for  $q=55.23 \text{ kW m}^{-2}$  and  $G=36.87 \text{ kg m}^{-2} \text{ s}^{-1}$  at  $0.016 \text{ s}$  time interval.

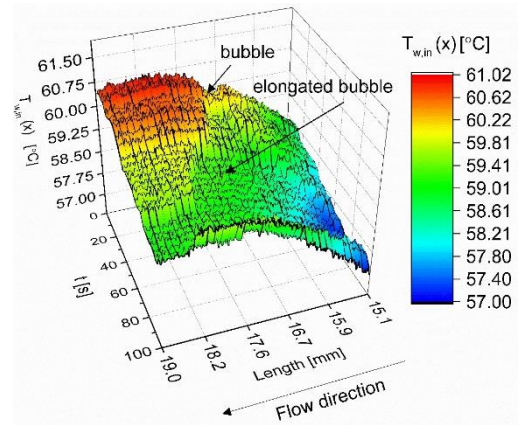


**Figure 4.** 3D plot of local inner wall temperature  $T_w$ , at the centreline vs time for  $G=23.59 \text{ kg m}^{-2} \text{ s}^{-1}$  and  $q=16.88 \text{ kW m}^{-2}$  from single bubble nucleation near the superheated sidewall and growth to elongated bubble.

### 4 Conclusions

Heat transfer coefficients in a single rectangular were calculated from interfacial temperature and local pressure data for the mass fluxes of  $23.59, 36.87, 73.74$  and  $101.62 \text{ kg m}^{-2} \text{ s}^{-1}$  and increasing heat fluxes, up to  $98 \text{ kW m}^{-2}$ . The local heat transfer coefficients during flow boiling was related to thermal images and flow observations. Heat transfer during single bubble growth and heat transfer deterioration was explained from the thermal images and flow visualisations. Heat transfer deterioration can be related to the liquid film thinning and subsequent dryout near the sidewalls of the channel after a vapour bubble occupies the whole channel cross section. This is associated with wall temperature rise.

### References

- [1] S. Gedupudi, Y. Q. Zu, T. G. Karayiannis, D. B. R. Kenning, and Y. Y. Yan, "Confined bubble growth during flow boiling in a mini/micro-channel of rectangular cross-section Part I: Experiments and 1-D modelling," *Int. J. Therm. Sci.*, vol. 50, no. 3, pp. 250–266, 2011.
- [2] Y. Wang and K. Sefiane, "Single bubble geometry evolution in micro-scale space," *Int. J. Therm. Sci.*, vol. 67, pp. 31–40, 2013.
- [3] S. Korniliou, C. Mackenzie-Dover, J. R. E. Christy, S. Harmand, A. J. Walton, and K. Sefiane, "Two-dimensional heat transfer coefficients with simultaneous flow visualisations during two-phase flow boiling in a PDMS microchannel," *Appl. Therm. Eng.*, vol. 130, 2018.